Molecular and Cellular Biochemistry
https://doi.org/10.1007/s11010-022-04588-w

Stability and expression of SARS-CoV-2 spike-protein mutations

Kristoffer T. Bæk[1] · Rukmankesh Mehra[2] · Kasper P. Kepp[1]

Received: 21 March 2022 / Accepted: 12 October 2022

Abstract

Protein fold stability likely plays a role in SARS-CoV-2 S-protein evolution, together with ACE2 binding and antibody evasion. While few thermodynamic stability data are available for S-protein mutants, many systematic experimental data exist for their expression. In this paper, we explore whether such expression levels relate to the thermodynamic stability of the mutants. We studied mutation-induced SARS-CoV-2 S-protein fold stability, as computed by three very distinct methods and eight different protein structures to account for method- and structure-dependencies. For all methods and structures used (24 comparisons), computed stability changes correlate significantly (99% confidence level) with experimental yeast expression from the literature, such that higher expression is associated with relatively higher fold stability. Also significant, albeit weaker, correlations were seen between stability and ACE2 binding effects. The effect of thermodynamic fold stability may be direct or a correlate of amino acid or site properties, notably the solvent exposure of the site. Correlation between computed stability and experimental expression and ACE2 binding suggests that functional properties of the SARS-CoV-2 S-protein mutant space are largely determined by a few simple features, due to underlying correlations. Our study lends promise to the development of computational tools that may ideally aid in understanding and predicting SARS-CoV-2 S-protein evolution.

Keywords SARS-CoV-2 · COVID-19 · Spike-protein · Mutations · Protein stability

Introduction

The pandemic caused by severe acute respiratory syndrome coronavirus 2 (SARS-CoV-2) [1–3] has led to intensive research into its spike-protein (S-protein, Fig. 1a), whose evolution may lead to changes in its surface that evade the human immune system [4–6]. The S-protein is a glycosylated homo-trimer on the surface of coronaviruses responsible for their characteristic shape [7, 8]. During entry of the virus particle into human host cells, the S-protein binds to the cell-surface receptor angiotensin-converting enzyme 2 (ACE2), Fig. 1b [9–11].

Due to the importance of S-protein epitopes for immune recognition, presentation of the S-protein is the rationale behind a range of important vaccines [12, 13]. The presence of prominent antibodies in a population may lead to selection pressure to change the S-protein surface to evade the antibodies learned from vaccination or infection with earlier variants [14]. Such antigenic drift may lead to variants capable of escaping vaccine-induced immunity, a problem that is likely to persist for many years. The omicron variant has been a hallmark example of such evolution, leading to a very large number of breakthrough infections in late 2021 and early 2022 [15].

Understanding such evolution effects requires protein structural data [16–19]. Since function is structure-dependent, the structure is the platform on which the amino acid evolution occurs, with evolution rates typically depending on the structural context of the amino acid site [20–22]. The recent technical breakthroughs in cryo-electron (cryo-EM) microscopy of large molecules [23–27] are an excellent example of basic science as essential for innovation, enabling publication of hundreds of SARS-CoV-2 S-protein structures during the pandemic both of the protein alone (apo-S-protein), in various conformation states, and in complex with a large range of antibodies and ACE2 at resolutions typically at 2–4 Å [28].

✉ Kasper P. Kepp
kpj@kemi.dtu.dk

Rukmankesh Mehra
rukmankesh@iitbhilai.ac.in

[1] DTU Chemistry, Technical University of Denmark, Building 206, 2800 Kongens Lyngby, Denmark

[2] Department of Chemistry, Indian Institute of Technology Bhilai, Sejbahar, Raipur 492015, Chhattisgarh, India

Published online: 27 October 2022

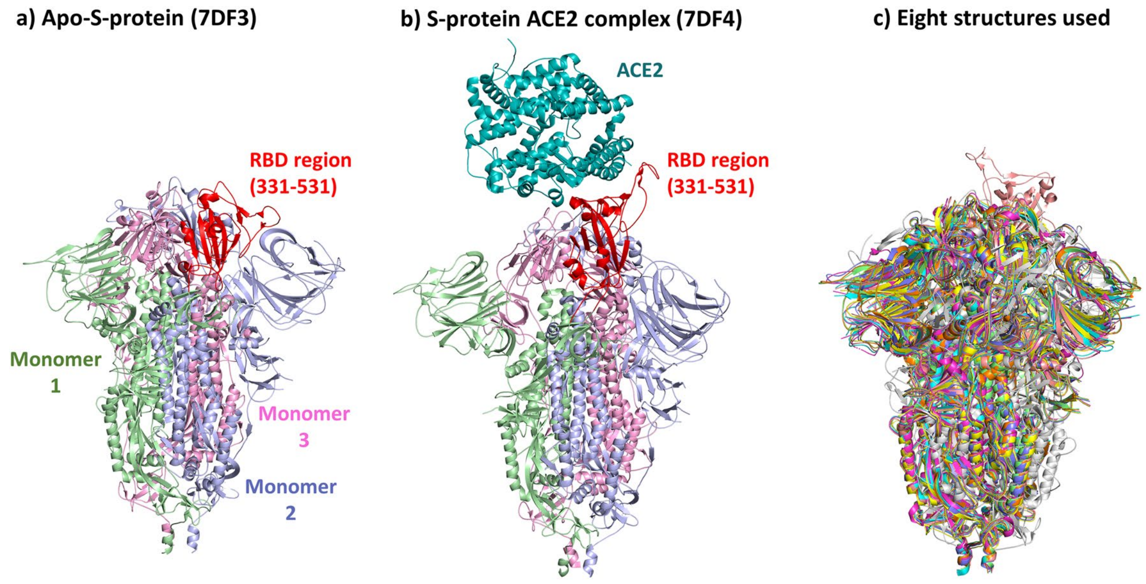

Fig.1 Structure of the SARS-CoV-2 S-protein, studied in this work. **a** Representative structure of the apo-S-protein state (PDB: 7DF3) [39] with the studied mutated sites of the RBD shown in red color. **b** Representative cryo-EM structure of the S-protein in complex with ACE2, (PDB: 7DF4). **c** Overlay of the eight prefusion S-protein structures used in this study to account for structural heterogeneity when computing mutation stability effects

Among the selection pressures acting on a protein beyond its direct function is the need to maintain the overall fold stability and translational fidelity, and thus evolution of new mutations often occurs with a tradeoff not to undermine these properties [17, 29–32]. Before fusion with a host cell, the S-protein is in a metastable conformation state under selection to evade antibodies and enhance ACE2 binding, which requires conversion to an “open” conformation state with the receptor binding domain (RBD) in an upward conformation state [33–37]. A new arising mutation with enhanced ACE2 binding or antibody evasion could affect epidemiology and clinical presentation (transmission / antigenic drift) but less likely so if the S-protein lost structural integrity. By conditioning the fitness space, stability function tradeoffs common to other aspects of protein evolution [29] may thus affect epidemiological and clinical relevance of new variants, an important topic even in the post-pandemic period [38].

Structure-based computational models based on machine learning or energy-based force fields can compute changes in protein stability upon mutation, [21, 40–47] and describe protein stability, antibody binding, and ACE2 binding for any possible mutation in the S-protein, using S-protein structures as input. If accurate, these models could then estimate the epidemiological (and perhaps clinical) impact of mutations, since transmission potential (reproduction numbers), incubation period, and virulence relate to these molecular properties of the virus [14, 48]. Unfortunately, there are major limitations to the accuracy of such methods [42, 49–55]. Good experimental data would help to train models suitable for predicting effects for new mutations where data are unavailable. The few experimental S-protein stability data from time-consuming differential scanning calorimetry or denaturation experiments prevent statistically meaningful analysis. Instead, we hypothesized that expression levels, available for very many SARS-CoV-2 S-protein mutations, may be a proxy of fold stability, as argued previously [56] and explored below for the first time.

Methods

Data for expression and ACE2 binding

Data for the effect of S-protein RBD single-point mutations on yeast expression and ACE2-binding were published by Starr et al. [56]. These mutation sites are marked in red color in Fig. 1a. The effect of mutations on expression is reported as the difference in log-mean fluorescence intensity (MFI) relative to wild-type (ΔlogMFI = logMFI$_{\text{variant}}$–logMFI$_{\text{wild-type}}$), such that a positive value indicates higher RBD expression [56]. The effect of mutations on ACE2-binding (Fig. 1b) is calculated from the apparent dissociation constants ($K_{D,\ app}$) and shown as the difference in log10($K_{D,app}$) relative to wild-type (Δlog10($K_{D,app}$) = log10($K_{D,app}$)$_{\text{wild-type}}$–log10($K_{D,app}$)$_{\text{variant}}$), such that a positive value indicates higher variant ACE2 binding [56]. There were two independent measurements (one from each of two independent libraries) for each mutation, providing an important way to assess the quality and reproducibility of the individual data points.

Data curation

There is an overall good correlation between the results obtained from the two independent libraries (Figure S1a). We removed outliers by filtering out observations where the two replicates are different (for binding *or* expression), defined as residuals > 1, or where data for one replicate is missing. The rationale is that data points not similar in the two experimental replicates cannot be considered reproduced and may erroneously affect analysis. We furthermore removed data points with effects on binding in either replicate < −4.5 to avoid values near the detection limit (see Figure S1a). The correlation between the replicates after curation is shown in Figure S1b. Removing outliers and data points at the detection limit also excluded stop codon mutations (Figure S2). The described curation removed 685 of the original 4221 data points. Further analyses were performed using the remaining 3536 data points and the average of the binding and expression data from the two independent libraries, with detailed data collected in the supplementary file Table_S1.csv.

Structures and computer models used to compute stability effects

For each mutation in the dataset, the change in protein free energy of folding (ΔΔG, kcal/mol) was computed using three different methods: The relatively new (2019) neural network method DeepDDG [57], the graph-based machine learning method mCSM [45] (mCSM), and the linear regression model SimBa-IB [58]. DeepDDG and mCSM were accessed via their respective web servers (http://protein.org.cn/ddg.html, http://biosig.unimelb.edu.au/mcsm/stability), and Simba-IB was run from the command-line (http://github.com/kasperplaneta/SimBa2). These data are available in the supplementary data file Table_S2.csv.

We have previously shown that analysis of functional properties can depend on input structure used, [59] and such heterogeneity is also seen in published cryo-EM structures of the S-protein [28]. Since our interest here is in exploring if computationally estimated stability changes of mutations correlate with experimental expression data of the prefusion S-protein, we used eight experimental cryo-EM structures of the prefusion S-protein from the Protein Data Bank (PDB) which reflect the state evaluated in the expression data better than an antibody or ACE2-bound state: 6VXX by Walls et al. [35], 6X6P by Herrera et al. [60], 6X79 by McCallum et al. [61], 6Z97 by Huo et al. [62], 6ZB4 by Toelzer et al. [63], 7CAB by Lv et al. [64], 7DDD by Zhang et al. [65], and 7DF3 by Zhang et al. [39] to account for such heterogeneity. Structural alignment of these eight structures using Schrodinger [66] indicates pairwise RMSD values of 0.64–3.10 Å. 7DDD and 7DF3 are made by the Shanghai group (Cong, Huang et al.), and 6VXX and 6X79 by Veesler's group; the others by different groups. All structures are closed, except 6Z97 having a partly open prefusion state for one of its RBDs. The structures are shown in structural overlay in Fig. 1c.

The relative solvent accessible surface area (RSA) of the mutated sites was calculated using SimBa-IB [58], which uses FreeSASA for this task [67]. Because the eight PDB structures represent homo-trimers, the ΔΔG and RSA values reported in this study are average ΔΔG and RSA values for the three chains (A, B, and C) of each structure.

It is important to note that the cryo-EM structures discussed may not reflect very precisely the real conformations of the S-protein at physiological temperature (37 °C): Cryo-EM structures are typically obtained with samples deposited with vitrified ice and rapidly cooled using a cryo-agent [24, 25, 68]. The freezing may remove some conformational dynamics [69–73]. Conformational changes of the S-protein may also be temperature-dependent [74]. In addition, the physiologically relevant state of the S-protein tends to be heavily glycosylated, which none of the experimental assays studying mutation impacts so far has addressed. Our goal is to identify whether experimental apo-S-protein data can be approximated by computed data, without translating these to the physiological significance of these data.

Results and discussion

Experimental and computed genotype–phenotype heat maps

Our main interest was to investigate whether experimentally measured expression and ACE2 binding of S-protein RBD mutants [56] can be related to the thermodynamic stability of the mutants. Amino acid substitutions often change the stability of a protein with a tendency for the distribution of such effects to be skewed toward destabilization [75]. Mutations in RBD affect expression of the S-protein and binding to ACE2 differently, but as discussed before [56], there is a relatively strong correlation ($R = 0.59$) between the effect of mutations on expression and ACE2 binding (Figure S3a). This relationship is not intuitive but could relate to underlying effects such as ACE2 recognition and stability both relating to the mutating site's solvent accessibility or correlations between codon use [76] which affects replication efficiency [77] and amino acid properties. Expression levels could also affect apparent binding constants even at the same specific ACE2 affinity, even if this is apparently accounted for, due

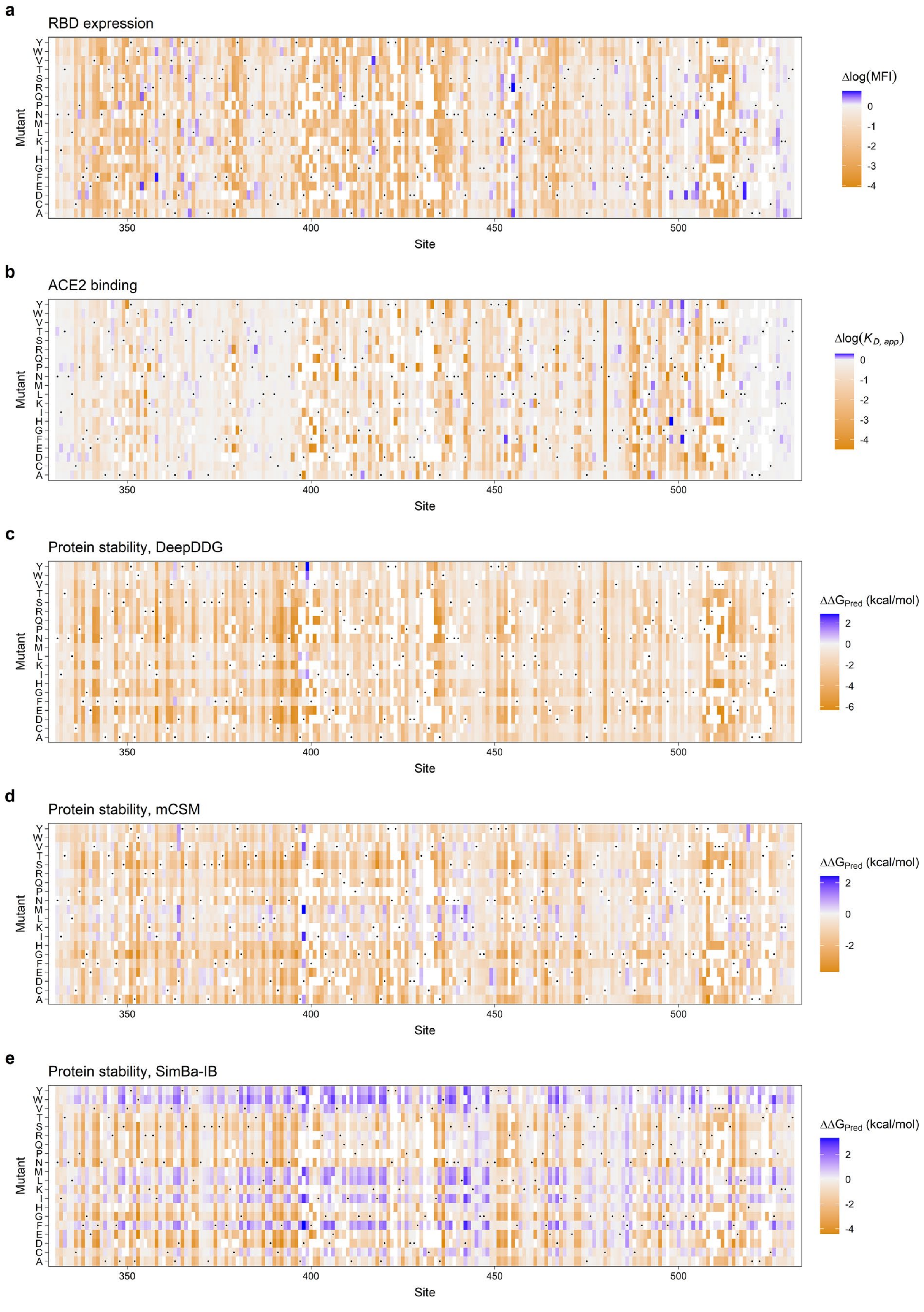
a
RBD expression
Δlog(MFI)
0
-1
-2
-3
-4
b
ACE2 binding
$\Delta\log(K_{D,\,app})$
0
-1
-2
-3
-4
c
Protein stability, DeepDDG
$\Delta\Delta G_{Pred}$ (kcal/mol)
2
0
-2
-4
-6
d
Protein stability, mCSM
$\Delta\Delta G_{Pred}$ (kcal/mol)
2
0
-2
e
Protein stability, SimBa-IB
$\Delta\Delta G_{Pred}$ (kcal/mol)
2
0
-2
-4
Mutant
Y W V T S R Q P N M L K I H G F E D C A
Site
350
400
450
500

◂**Fig. 2** Heat maps of mutation effects on RBD experimental expression and ACE2 binding (from Starr et al. [56]) compared with computed stability change (this work). **a** expression; **b** ACE2-binding affinity. Protein stability change computed with: (**c**) deepDDG; **d** mCSM **e** SimBa-IB. Rectangles are colored by mutational effect according to scale bars on the right. Black dots indicate the wild-type residues. White rectangles represent mutations for which there is no data in the curated dataset

to complex (e.g., tertiary) interactions. The large number of mutations having a small or "nearly neutral" impact, as noted by the authors [56] and reasonably expected, may also spuriously affect the relationships. However, if the data are grouped to adjust for the skewed distribution, the correlation between expression and binding becomes even larger and quite remarkable ($R = 0.88$) (Figure S3b).

To assess the correlation between the effects of mutations on expression, ACE2 binding and protein stability, we computationally predicted the stability changes (ΔΔG) caused by the mutations in RBD using three state-of-the-art methods (DeepDDG, mCSM, and SimBa-IB) and compared with the experimentally observed changes in expression and binding. Figure 2a, b shows heat maps build from the experimental data by Starr et al. [56] after curation for non-reproducible replicates as described in Methods. These experimental heat maps are compared with the computational heat maps of ΔΔG derived in the present work, using DeepDDG (Fig. 2c), mCSM (Fig. 2d), and SimBa-IB (Fig. 2e). SimBa produces more stabilizing trends overall, as it was developed to handle destabilization biases. (The method performs similarly to other methods in benchmarks despite this feature.) [49, 58]

The heat maps in Fig. 2 of experimental binding and expression do have some residual similarities, as also mentioned by Starr et al. [56]. The computed stability effects provide estimates of the impact of all possible mutations in the RBD, and show some similarities to the expression data, notably with nearly neutral effects (gray) being common to both experimental and computed data in the N- and C-terminals and in some regions of the protein around 444–450 and a larger area around 470–488. In contrast, mutations in the region 388–396 have strong effects on protein stability but are nearly neutral with respect to expression and ACE2 binding. Overall, there is less similarity between ACE2 binding and the computed stability changes as perhaps expected.

RBD sites with non-neutral effects cluster in the structured regions

Figure 3 shows the effect of mutation at each site on expression, ACE2 binding and predicted protein stability mapped onto the RBD structure. The effect at each site is calculated as the average of the absolute effect (without sign) of all 19 mutations as a measure of the tolerance to mutation at each site. Mutations that affect expression are mainly located in the core RBD subdomain, and in particular in the central beta sheet and its flanking alpha helices (Fig. 3a). Mutations that affect binding are located in the ACE2 binding subdomain or, similarly to mutations that affect expression, in the central beta sheet, while large parts of the RBD domain are tolerant to mutations with regard to ACE2 binding (Fig. 3b). Mutations that affect protein stability are mainly located in the structured core of the RBD subdomain, similarly to the effect of mutations on expression (Fig. 3c–e). When evaluating the computational methods in this way, their ability to identify the most tolerant sites for mutation (or equally, the sites more likely to be neutral from an evolutionary perspective) becomes more evident than in the heat maps of Fig. 2, while the better agreement with expression remains clear.

Computed and experimental S-protein mutant properties correlate significantly

As discussed above, mutations in the RBD affect expression, ACE2 binding and protein stability differently, but with some overlap in site effects especially for protein stability and expression. To quantify this relationship, we plotted the predicted ΔΔG values for all mutations against the observed changes in RBD expression (Fig. 4a) and ACE2 binding (Fig. 4b), respectively, for each experimental structure used as input for the three methods (24 comparisons for all studied RBD mutations for expression and 24 comparisons for ACE2 binding). Correlations between RBD expression and ΔΔG for individual PDB structures are consistently observed, but their magnitude depends on the prediction method, with correlation coefficients ranging from 0.40 to 0.48 for DeepDDG, 0.27 to 0.34 for mCSM, and 0.12 to 0.22 for SimBa-IB (Fig. 4a).

The observed ACE2 binding and the predicted ΔΔG also correlate, depending on the prediction method (Fig. 4b), which is in line with the correlation between experimental measures of expression and ACE2 binding (Figure S3). However, the correlations are weaker than for expression with correlation coefficients ranging from 0.29 to 0.37 for DeepDDG, 0.13 to 0.26 for mCSM, and 0.09 to 0.15 for SimBa-IB. In all 48 comparisons of computed and experimental data in Fig. 4, the correlations are statistically significant at the 99% confidence level (p-values of linear regression < 0.01).

Figure 5 shows the aggregate data for all structures, to account for structural heterogeneity effects. The relationships observed in Fig. 4 still hold true when averaging over all eight structures, i.e., our result is robust to structural heterogeneity. The effect of mutations on protein stability predicted using DeepDDG correlates better with both expression and ACE2 binding than using mCSM and especially SimBa-IB (Figs. 4 and 5). Judging from Fig. 3c–e, the three methods agree to a large extent on how they predict the

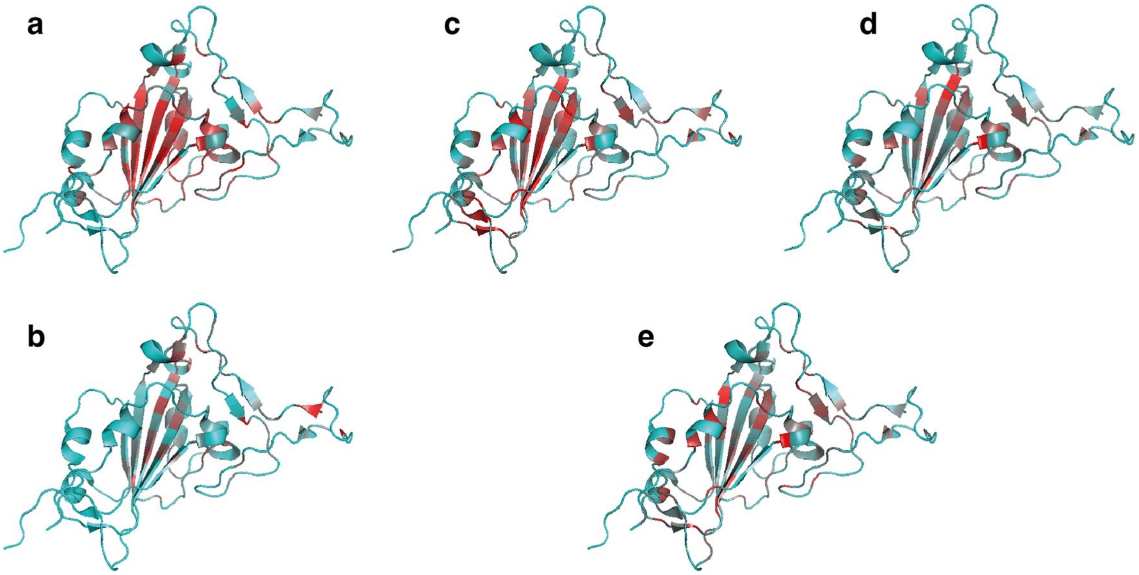

Fig. 3 Effects of mutations mapped onto the SARS-CoV-2 RBD structure. Each residue is color-coded from cyan to red according to the average absolute effects of mutation. **a** RBD expression. **b** ACE2 binding. **c** Protein stability estimated by DeepDDG. **d** Protein stability estimated by mCSM, and **e** Protein stability estimated by SimBaIB. Cyan indicates no effect, red indicates a strong effect. The color scales are relative within each panel. The ACE2 binding motif is shown on the right-hand side in each structure. (PDB: 6Z97, Chain A)

tolerability of a site to mutation, whereas they differ in how they predict the effect of individual mutations (Fig. 2c–e), and this is most likely the cause of the differences in the resulting correlations.

Both the binding and expression effects are highly skewed, with an overrepresentation of data points between 0 and −1 (Figure S2). In order to adjust for this, we grouped the data into bins of 0.5-width and 0.25-width and calculated the mean expression and binding effect in each bin, and the mean predicted ΔΔG value for each bin. Figure 6 shows these data as averages of all PDBs (data for individual structures in Figures S4–S7). The correlation increases substantially upon binning, with each data point more well-determined, whereas the *p*-values decrease substantially due to the few aggregate data points after averaging. Remarkably, the computational data correlate extremely well with the binned experimental data, especially for DeepDDG, much more than normally seen [49]. Considering that the models were developed to predict fold stability effects, not expression (which also depends on effects at the nucleic acid level) and that we used the full S-protein structures, whereas the experiments express RBD on the yeast surface with expected modifications, this result is very surprising. One interpretation of this result is that broader functional properties of the mutant space of the S-protein are in fact largely determined by a few simple features, due to underlying correlations.

To understand the correlations on a per-site basis, Fig. 7 shows the relationships between the experimental and computed data averaged over sites, as an indicator of the site's tolerance to mutations. As this removes some amino acid specific variations between the three computer models used, the correlations now become more similar between the methods. In all cases, there is a significant correlation (99% confidence level, *p*-values of linear regression), such that sites more neutral to expression and ACE2 binding effects experimentally are also more neutral toward computed stability effects.

As shown in Figure S8, the three methods when applied to the same structures show generally good correlations, with $R = 0.55$–0.68, i.e., they have a large overlap in their description of the general trends in the total data set. Still, deepDDG is a clearly better method for estimating the experimental data, especially the expression data (Figs. 4, 5, 6), although the reasons can be several (it is a neural network method trained on > 5000 data points; [57] SimBa is a simpler linear regression model, [58, 78], and mCSM, a graph-based machine learning method, is somewhat older [45]).

Mutations in residues that are buried in the core of a protein tend to have larger effect on protein stability, which is also the case for the RBD domain, where mutations in the core subdomain are less tolerated (Fig. 3c–e) than mutations near the surface. To quantify if surface exposure of residues in RBD correlated with the effect of the mutations on expression and binding, we plotted these variables against the RSA for each site, and we see a moderate correlation ($R = 0.29$ for binding, and $R = 0.43$ for expression) with a notable overall tolerance to mutation at sites with high solvent exposure (Figure S9). As expected, there is also a good

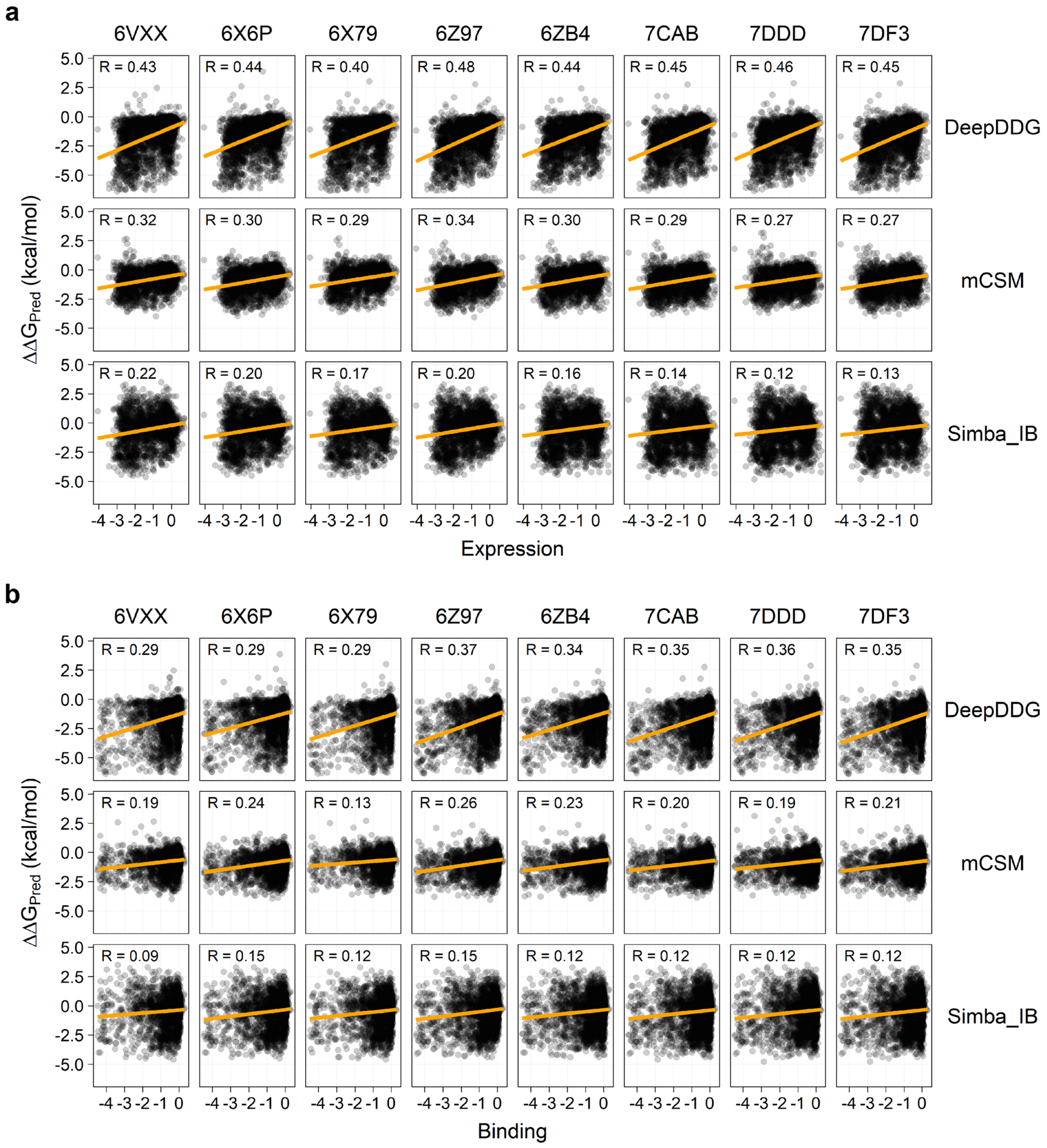

Fig. 4 Predicted change in protein stability as a function of mutations effect on RBD expression and ACE2 binding. Three different prediction methods (DeepDDG, mCSM, and SimBa-IB; indicated on the right) were used to predict the change in protein stability for each mutation using eight different experimental structures of the S-protein (indicated on top). Orange lines indicate the resulting linear regression, and the correlation coefficients (R) are shown. The *p*-values for all correlations are < 0.001. **a** ΔΔG plotted against RBD expression, and **b** ΔΔG plotted against ACE2 binding

correlation between surface exposure and predicted stability changes, with correlation coefficients ranging from 0.27 (for SimBa-IB) to 0.60 (for DeepDDG; Figure S10).

Whereas enough data points required for statistical analysis are available for expression, there are a few good studies studying directly the turnover/stability of selected

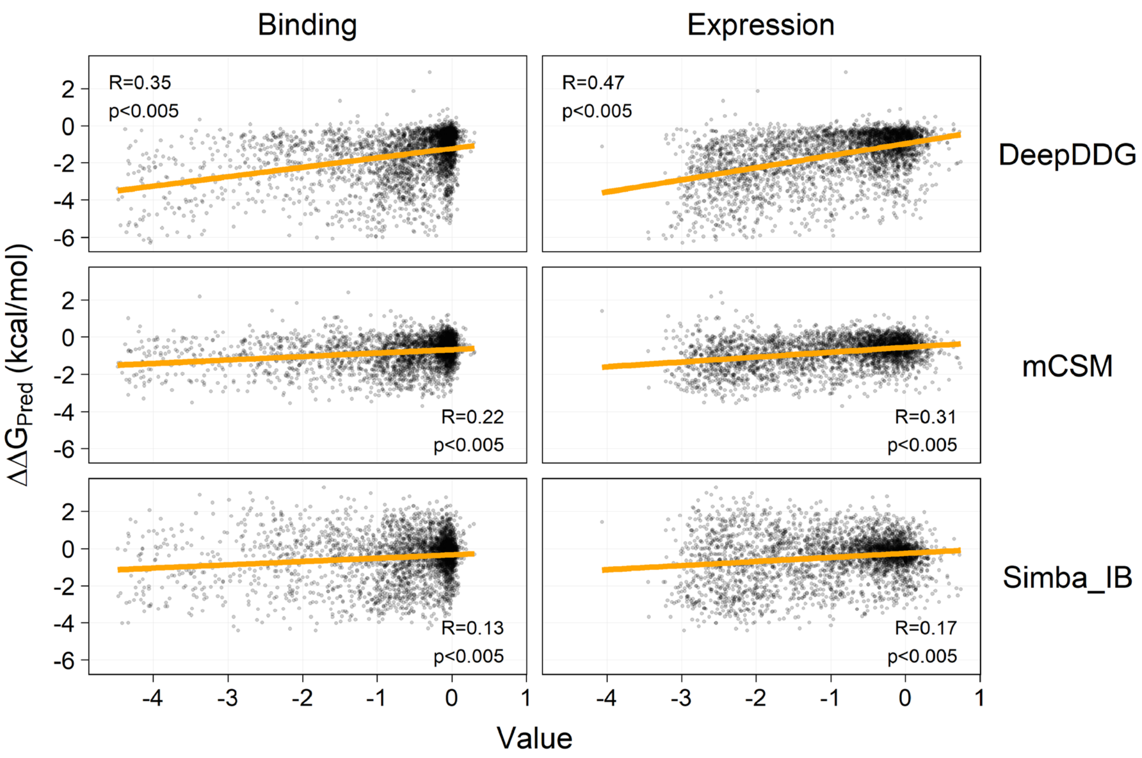

Fig. 5 Average change in protein stability for the eight used structures vs. effect on RBD expression and ACE2 binding. Stability changes upon mutation for DeepDDG, mCSM, and SimBa-IB correlate with the experimental data at 99% significance (*p*-values of linear regression). Orange lines indicate the resulting linear regression

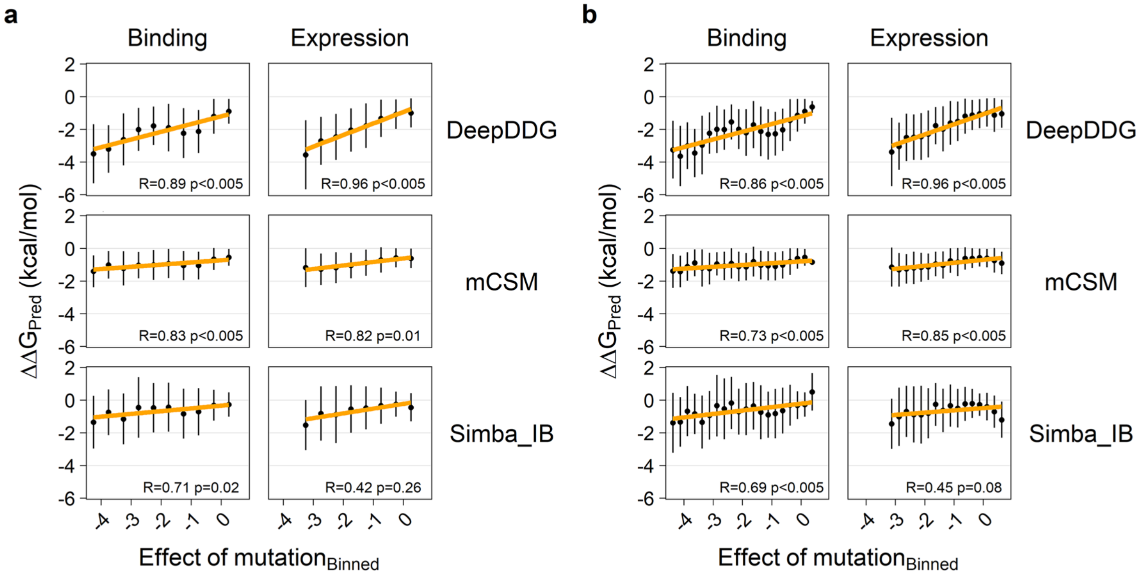

Fig. 6 Predicted change in protein stability as a function of mutations effect on RBD expression and binding to ACE2 using binned data. Three different prediction methods (DeepDDG, mCSM, and SimBa-IB) were used to predict the change in protein stability for each mutation using eight different experimental structures of Spike-protein. The average change in stability for the eight structures is used in the calculation. **a** Binding and expression data grouped in 0.5-value bins **b** Binding and expression data grouped in 0.25-value bins

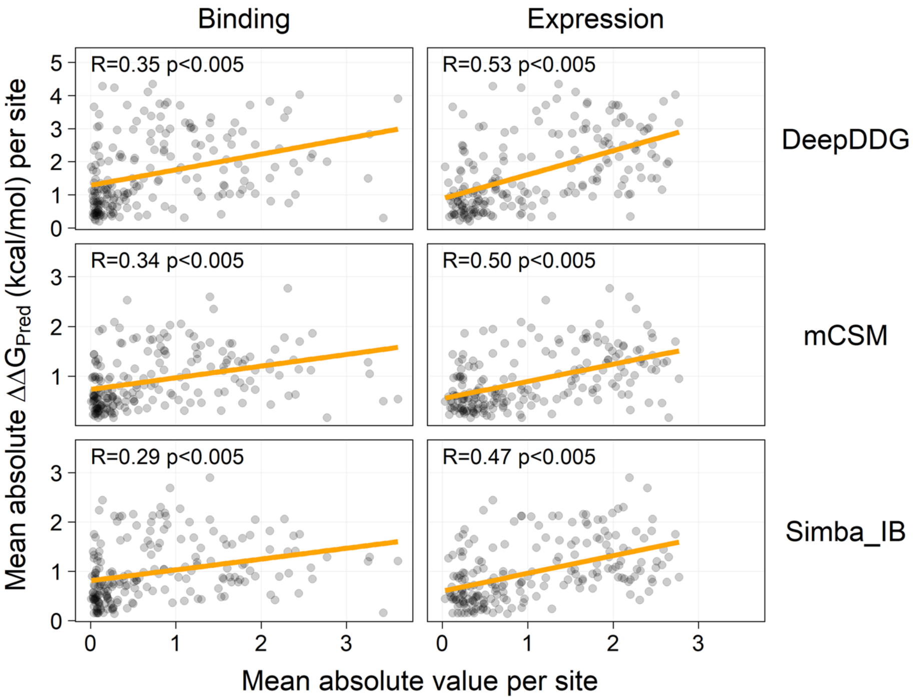

Fig. 7 Site-averaged impact on ACE2 binding and expression vs. stability changes. This figure shows experimental-computational relationships for site-averaged properties (all mutations with data for each site-averaged) as an indicator of the site's tolerance to mutation

mutations. Barrett et al. provided data on D614G, A831V, D839Y/N/E, S943P, and P1263L, showing diverse fusion effects but turnover/stability mostly similar to the reference Wuhan strain [79]. Although our study focuses on RBD mutations as in the experimental assays, this agrees well with $\Delta\Delta G = -0.4$ kcal/mol for D614G and -0.1 kcal/mol for S943P (using SimBa; sites 831 and 839 and 1263 not being available in the 6X6P structure used for this estimate; average stability effect of all possible mutations -1.2 kcal/mol, destabilizing). However, there are too few data to make these comparisons statistically significant and agreement could be coincidental.

Also of interest, Teng et al. [80] investigated S-protein mutation stability effects exhaustively using other models (FoldX primarily), however without validation against experimental data. Still, the cited relatively small stabilization effect for D614G in that study is reasonably consistent with the experiments by Barrett et al. [79] given the uncertainty in computations and experimental data, but in contrast to another computational study comparing many computer models, but finding D614G destabilizing [81]. As computational estimates for single mutations can thus vary, broader benchmarking of groups of mutations against many experimental data, as here, may be necessary.

A major limitation moving forward on computational structure-based SARS-CoV-2 evolution is the in vivo relevance of the cryo-EM structures used as input and the in vitro protein states using to generate the experimental data, as the S-protein is heavily glycosylated [82]. Another major limitation specific to single-mutation data (both experimental and computational) is epistasis modulating the impact of mutation effects when multiple mutations are present together [83]. These limitations are in addition to those of wild-type-structure-based computer models extrapolating effects to a mutant protein state [42, 50, 51, 58]. Also, pathogens with many proteins contributing to fitness and phenotype, e.g., bacteria, would require models for many proteins, posing additional major challenges.

Concluding remarks and biological implications

The SARS-CoV-2 S-protein fusion with human ACE2 is a prerequisite for host cell entry [9, 10]. However, S-protein antibodies induced by previous infection or vaccines bind the S-protein and neutralize some virus particles, thus reducing infectivity. During evolution of SARS-CoV-2, these two effects are under selection [28]. Most SARS-CoV-2 evolution until the omicron variant involved selection for better ACE2 binding [84], whereas omicron reflects substantial evasion of existing antibodies via its many mutations in the S-protein [85]. In addition to these two effects, protein fold stability is an important constraint on protein evolution of new functionality (function-stability tradeoffs) [29, 30, 86, 87] and may play a role in SARS-CoV-2 S-protein evolution as well [28]. In order to understand and possibly predict SARS-CoV-2 evolution, an important health challenge, [28, 38] we explored if computer models can predict experimental mutant expression data, as a proxy of stability.

Our work shows that computed protein stability effects correlate significantly for all 48 comparisons of data sets (eight structures, three methods, and two properties) with expression levels and to lesser extent ACE2 binding observed in experiments [56]. The correlations between ACE2 binding and expression may reflect underlying correlations to codon use, amino acid chemical properties, and site solvent exposure. Such correlations could impact the mutability of the SARS-CoV-2 S-protein and affect phenotype tradeoffs, and thus ultimately virus evolution, given that S-protein fold stability in the prefusion state is important [28, 33]. To the extent that protein stability maintenance is important, it will affect SARS-CoV-2 S-protein evolution via constraints on antigenic drift.

Single amino acid changes as analyzed above and in assays [88, 89] are unlikely to be fully additive in variants with multiple substitutions, due to amino acid correlations (a form of intra-gene epistasis), and possibly epistasis with other virus genes [83, 90–92]. These epistasis effects haunt the protein evolution field and are not easily accounted for, but recent work suggests that substantial parts of the epistasis is already utilized, [93] although this remains to be studied in future work, and does not include potential inter-gene epistasis such as processing of S-protein RNA by non-structural proteins during virus replication within the host cell. Still, the maintenance of S-protein fold stability in the lipid surface of the virion is likely to be an important constraint on ACE2 binding and antigenic drift making the heat maps studied here of interest both as a proxy of expression and S-protein stability but possibly also as a contribution to computational estimates of the fitness function of SARS-CoV-2.

Our work represents the first benchmark of computer models against a large experimental data set of S-protein mutation effects. The finding that expression data correlate to computationally estimated stability effects suggests that computer models may estimate the stability/expression effects of new mutations for which we do not have data, although many challenges remain, as described. If and only if these challenges are addressed, appropriate models could perhaps eventually help to rationalize from the molecular impact of the amino acid changes to the observable characteristics of the virus, including its epidemiology.

Supplementary Information The online version contains supplementary material available at https://doi.org/10.1007/s11010-022-04588-w.

Author contributions KTB collected and curated the data, developed the scripts and performed the main analysis. KTB, RM, and KPK analyzed the data. KTB, RM, and KPK wrote the paper. KPK and KTB planned the work. All authors read and approved the final manuscript.

Funding The Danish Council for Independent Research (Grant case: 8022-00041B) is gratefully acknowledged for supporting this work.

Data availability The full curated data used in this study are available as a csv file uploaded as supplementary information (Table_S1.csv and Table_S2.csv), and scripts for analyzing these data are available at the web page https://github.com/ktbaek/Spike-ACE2.

Declarations

Competing interests The authors declare no competing interests.

Conflict of interest The authors declare no conflicts of interest, financial or otherwise, associated with this work.

References

1. Wu F, Zhao S, Yu B et al (2020) A new coronavirus associated with human respiratory disease in China. Nature 579:265–269
2. Zhu N, Zhang D, Wang W et al (2020) A novel coronavirus from patients with pneumonia in China, 2019. N Engl J Med 382:727–733
3. Cevik M, Kuppalli K, Kindrachuk J, Peiris M (2020) Virology, transmission, and pathogenesis of SARS-CoV-2. BMJ. https://doi.org/10.1136/bmj.m3862
4. Dejnirattisai W, Zhou D, Ginn HM et al (2021) The antigenic anatomy of SARS-CoV-2 receptor binding domain. Cell 184:2183-2200.e22. https://doi.org/10.1016/j.cell.2021.02.032
5. Kemp SA, Collier DA, Datir RP et al (2021) SARS-CoV-2 evolution during treatment of chronic infection. Nature 592:277–282. https://doi.org/10.1038/s41586-021-03291-y
6. van Dorp L, Houldcroft CJ, Richard D, Balloux F (2021) COVID-19, the first pandemic in the post-genomic era. Curr Opin Virol 50:40–48
7. Harvey WT, Carabelli AM, Jackson B et al (2021) SARS-CoV-2 variants, spike mutations and immune escape. Nat Rev Microbiol 19:409–424
8. Guruprasad L (2021) Human SARS CoV-2 spike protein mutations. Proteins Struct Funct Bioinforma 89:569–576. https://doi.org/10.1002/prot.26042
9. Letko M, Marzi A, Munster V (2020) Functional assessment of cell entry and receptor usage for SARS-CoV-2 and other lineage B betacoronaviruses. Nat Microbiol 5:562–569
10. Fehr AR, Perlman S (2015) Coronaviruses: an overview of their replication and pathogenesis. Coronaviruses Methods Protoc. Springer, New York, pp 1–23
11. Wang Q, Zhang Y, Wu L et al (2020) Structural and functional basis of SARS-CoV-2 entry by using human ACE2. Cell 181:894–904
12. Liu C, Zhou Q, Li Y et al (2020) Research and development on therapeutic agents and vaccines for COVID-19 and related human coronavirus diseases. ACS Cent Sci 6(3):315–331
13. Forni G, Mantovani A (2021) COVID-19 vaccines: where we stand and challenges ahead. Cell Death Differ 28:626–639
14. Yuan M, Huang D, Lee C-CD et al (2021) Structural and functional ramifications of antigenic drift in recent SARS-CoV-2 variants. Science 373:818–823. https://doi.org/10.1126/science.abh1139
15. Liu L, Iketani S, Guo Y et al (2022) Striking antibody evasion manifested by the Omicron variant of SARS-CoV-2. Nature 602:676–681
16. Dasmeh P, Serohijos AWR, Kepp KP, Shakhnovich EI (2013) Positively selected sites in cetacean myoglobins contribute to protein stability. PLoS Comput Biol 9:e1002929
17. Liberles DA, Teichmann SA, Bahar I et al (2012) The interface of protein structure, protein biophysics, and molecular evolution. Protein Sci 21:769–785. https://doi.org/10.1002/pro.2071

18. Bajaj M, Blundell T (1984) Evolution and the tertiary structure of proteins. Annu Rev Biophys Bioeng 13:453–492
19. Wylie CS, Shakhnovich EI (2011) A biophysical protein folding model accounts for most mutational fitness effects in viruses. Proc Natl Acad Sci U S A 108:9916–9921. https://doi.org/10.1073/pnas.1017572108
20. Drummond DA, Wilke CO (2008) Mistranslation-induced protein misfolding as a dominant constraint on coding-sequence evolution. Cell 134:341–352. https://doi.org/10.1016/j.cell.2008.05.042
21. Topham CM, Srinivasan N, Blundell TL (1997) Prediction of the stability of protein mutants based on structural environment-dependent amino acid substitution and propensity tables. Protein Eng 10:7–21
22. Worth CL, Gong S, Blundell TL (2009) Structural and functional constraints in the evolution of protein families. Nat Rev Mol Cell Biol 10:709
23. Blundell TL, Chaplin AK (2021) The resolution revolution in X-ray diffraction, Cryo-EM and other technologies. Prog Biophys Mol Biol 160:2–4. https://doi.org/10.1016/j.pbiomolbio.2021.01.003
24. Murata K, Wolf M (2018) Cryo-electron microscopy for structural analysis of dynamic biological macromolecules. Biochim Biophys Acta—Gen Subj 1862:324–334. https://doi.org/10.1016/j.bbagen.2017.07.020
25. Fernandez-Leiro R, Scheres SHW (2016) Unravelling biological macromolecules with cryo-electron microscopy. Nature 537:339–346. https://doi.org/10.1038/nature19948
26. Danev R, Yanagisawa H, Kikkawa M (2019) Cryo-electron microscopy methodology: current aspects and future directions. Trends Biochem Sci 44:837–848
27. Elmlund D, Elmlund H (2015) Cryogenic electron microscopy and single-particle analysis. Annu Rev Biochem 84:499–517
28. Mehra R, Kepp KP (2022) Structure and mutations of SARS-CoV-2 spike protein: a focused overview. ACS Infect Dis 8:29–58. https://doi.org/10.1021/acsinfecdis.1c00433
29. Tokuriki N, Stricher F, Serrano L, Tawfik DS (2008) How protein stability and new functions trade off. PLoS Comput Biol. https://doi.org/10.1371/journal.pcbi.1000002
30. Goldstein RA (2011) The evolution and evolutionary consequences of marginal thermostability in proteins. Proteins 79:1396–1407. https://doi.org/10.1002/prot.22964
31. Kepp KP (2020) Survival of the cheapest: how proteome cost minimization drives evolution. Q Rev Biophys. https://doi.org/10.1017/S0033583520000037
32. Bershtein S, Goldin K, Tawfik DS (2008) Intense neutral drifts yield robust and evolvable consensus proteins. J Mol Biol 379:1029–1044. https://doi.org/10.1016/j.jmb.2008.04.024
33. Berger I, Schaffitzel C (2020) The SARS-CoV-2 spike protein: balancing stability and infectivity. Cell Res 30:1059–1060. https://doi.org/10.1038/s41422-020-00430-4
34. Cai Y, Zhang J, Xiao T et al (2020) Distinct conformational states of SARS-CoV-2 spike protein. Science 369:1586–1592
35. Walls AC, Park Y-J, Tortorici MA et al (2020) Structure, function, and antigenicity of the SARS-CoV-2 spike glycoprotein. Cell 181:281–292
36. Henderson R, Edwards RJ, Mansouri K et al (2020) Controlling the SARS-CoV-2 spike glycoprotein conformation. Nat Struct Mol Biol 27:925–933. https://doi.org/10.1038/s41594-020-0479-4
37. Wrapp D, Wang N, Corbett KS et al (2020) Cryo-EM structure of the 2019-nCoV spike in the prefusion conformation. Science 367:1260–1263. https://doi.org/10.1126/science.abb2507
38. Maher MC, Bartha I, Weaver S et al (2022) Predicting the mutational drivers of future SARS-CoV-2 variants of concern. Sci Transl Med. https://doi.org/10.1126/scitranslmed.abk3445
39. Xu C, Wang Y, Liu C et al (2021) Conformational dynamics of SARS-CoV-2 trimeric spike glycoprotein in complex with receptor ACE2 revealed by cryo-EM. Sci Adv. https://doi.org/10.1126/sciadv.abe5575
40. Kulshreshtha S, Chaudhary V, Goswami GK, Mathur N (2016) Computational approaches for predicting mutant protein stability. J Comput Aided Mol Des 30:401–412
41. Montanucci L, Savojardo C, Martelli PL et al (2019) On the biases in predictions of protein stability changes upon variations: the INPS test case. Bioinformatics 35:2525–2527
42. Pucci F, Bernaerts KV, Kwasigroch JM, Rooman M (2018) Quantification of biases in predictions of protein stability changes upon mutations. Bioinformatics 34:3659–3665. https://doi.org/10.1093/bioinformatics/bty348
43. Potapov V, Cohen M, Schreiber G (2009) Assessing computational methods for predicting protein stability upon mutation: good on average but not in the details. Protein Eng Des Sel 22:553–560. https://doi.org/10.1093/protein/gzp030
44. Worth CL, Preissner R, Blundell TL (2011) SDM–a server for predicting effects of mutations on protein stability and malfunction. Nucleic Acids Res 39:W215–W222. https://doi.org/10.1093/nar/gkr363
45. Pires DEV, Ascher DB, Blundell TL (2014) MCSM: Predicting the effects of mutations in proteins using graph-based signatures. Bioinformatics 30:335–342. https://doi.org/10.1093/bioinformatics/btt691
46. Dehouck Y, Grosfils A, Folch B et al (2009) Fast and accurate predictions of protein stability changes upon mutations using statistical potentials and neural networks: PoPMuSiC-2.0. Bioinformatics 25:2537–2543. https://doi.org/10.1093/bioinformatics/btp445
47. Capriotti E, Fariselli P, Casadio R (2005) I-Mutant2.0: predicting stability changes upon mutation from the protein sequence or structure. Nucleic Acids Res 33:W306–W310
48. Han P, Li L, Liu S et al (2022) Receptor binding and complex structures of human ACE2 to spike RBD from omicron and delta SARS-CoV-2. Cell 185:630–640
49. Pucci F, Schwersensky M, Rooman M (2022) Artificial intelligence challenges for predicting the impact of mutations on protein stability. Curr Opin Struct Biol 72:161–168. https://doi.org/10.1016/j.sbi.2021.11.001
50. Casadio R, Savojardo C, Fariselli P et al (2022) Turning failures into applications: The problem of protein ΔΔG prediction. In: Carugo Oliviero, Eisenhaber Frank (eds) Data Min Tech Life Sci. Springer, Berlin, pp 169–185
51. Caldararu O, Mehra R, Blundell TL, Kepp KP (2020) Systematic investigation of the data set dependency of protein stability predictors. J Chem Inf Model 60:4772–4784. https://doi.org/10.1021/acs.jcim.0c00591
52. Christensen NJ, Kepp KP (2012) Accurate stabilities of laccase mutants predicted with a modified FoldX protocol. J Chem Inf Model 52:3028–3042. https://doi.org/10.1021/ci300398z
53. Kepp KP (2014) Computing stability effects of mutations in human superoxide dismutase 1. J Phys Chem B 118:1799–1812. https://doi.org/10.1021/jp4119138
54. Kepp KP (2015) Towards a “Golden Standard” for computing globin stability: stability and structure sensitivity of myoglobin mutants. Biochim Biophys Acta 1854:1239–1248. https://doi.org/10.1016/j.bbapap.2015.06.002
55. Thiltgen G, Goldstein RA (2012) Assessing predictors of changes in protein stability upon mutation using self-consistency. PLoS ONE. https://doi.org/10.1371/journal.pone.0046084
56. Starr TN, Greaney AJ, Hilton SK et al (2020) Deep mutational scanning of SARS-CoV-2 receptor binding domain reveals constraints on folding and ACE2 binding. Cell 182:1295–1310
57. Cao H, Wang J, He L et al (2019) DeepDDG: predicting the stability change of protein point mutations using neural networks. J Chem Inf Model 59:1508–1514

58. Bæk KT, Kepp KP (2022) Data set and fitting dependencies when estimating protein mutant stability: toward simple, balanced, and interpretable models. J Comput Chem 43:504–518. https://doi.org/10.1002/jcc.26810
59. Caldararu O, Blundell TL, Kepp KP (2021) A base measure of precision for protein stability predictors: structural sensitivity. BMC Bioinformatics 22:88. https://doi.org/10.1186/s12859-021-04030-w
60. Herrera NG, Morano NC, Celikgil A et al (2021) Characterization of the SARS-CoV-2 S protein: biophysical, biochemical, structural, and antigenic analysis. ACS Omega 6:85–102. https://doi.org/10.1021/acsomega.0c03512
61. McCallum M, Walls AC, Bowen JE et al (2020) Structure-guided covalent stabilization of coronavirus spike glycoprotein trimers in the closed conformation. Nat Struct Mol Biol 27:942–949. https://doi.org/10.1038/s41594-020-0483-8
62. Huo J, Zhao Y, Ren J et al (2020) Neutralization of SARS-CoV-2 by destruction of the prefusion spike. Cell Host Microbe 28:445-454.e6. https://doi.org/10.1016/j.chom.2020.06.010
63. Toelzer C, Gupta K, Yadav SKN et al (2020) Free fatty acid binding pocket in the locked structure of SARS-CoV-2 spike protein. Science 370:725–730. https://doi.org/10.1126/science.abd3255
64. Lv Z, Deng Y-Q, Ye Q et al (2020) Structural basis for neutralization of SARS-CoV-2 and SARS-CoV by a potent therapeutic antibody. Science 369:1505–1509. https://doi.org/10.1126/science.abc5881
65. Zhang C, Wang Y, Zhu Y et al (2021) Development and structural basis of a two-MAb cocktail for treating SARS-CoV-2 infections. Nat Commun 12:1–16
66. Schrödinger Release 2022-3: Maestro, Schrödinger, LLC, New York, NY (2021)
67. Mitternacht S (2016) FreeSASA an open source C library for solvent accessible surface area calculations. F1000Res. https://doi.org/10.12688/f1000research.7931.1
68. Meents A, Gutmann S, Wagner A, Schulze-Briese C (2010) Origin and temperature dependence of radiation damage in biological samples at cryogenic temperatures. Proc Natl Acad Sci 107:1094–1099
69. Mehra R, Dehury B, Kepp KP (2020) Cryo-temperature effects on membrane protein structure and dynamics. Phys Chem Chem Phys 22:5427–5438
70. Linden AH, Franks WT, Akbey Ü et al (2011) Cryogenic temperature effects and resolution upon slow cooling of protein preparations in solid state NMR. J Biomol NMR 51:283–292. https://doi.org/10.1007/s10858-011-9535-z
71. Tilton RF Jr, Dewan JC, Petsko GA (1992) Effects of temperature on protein structure and dynamics: X-ray crystallographic studies of the protein ribonuclease-a at nine different temperatures from 98 to 320K. Biochemistry 31:2469–2481
72. Doster W, Bachleitner A, Dunau R et al (1986) Thermal properties of water in myoglobin crystals and solutions at subzero temperatures. Biophys J 50:213–219. https://doi.org/10.1016/S0006-3495(86)83455-5
73. Dunlop KV, Irvin RT, Hazes B (2005) Pros and cons of cryocrystallography: should we also collect a room-temperature data set? Acta Crystallogr Sect D Biol Crystallogr 61:80–87
74. Edwards RJ, Mansouri K, Stalls V et al (2021) Cold sensitivity of the SARS-CoV-2 spike ectodomain. Nat Struct Mol Biol 28:128–131
75. Tokuriki N, Stricher F, Schymkowitz J et al (2007) The stability effects of protein mutations appear to be universally distributed. J Mol Biol 369:1318–1332. https://doi.org/10.1016/j.jmb.2007.03.069
76. Kandeel M, Ibrahim A, Fayez M, Al-Nazawi M (2020) From SARS and MERS CoVs to SARS-CoV-2: Moving toward more biased codon usage in viral structural and nonstructural genes. J Med Virol 92:660–666. https://doi.org/10.1002/jmv.25754
77. Hanson G, Coller J (2018) Codon optimality, bias and usage in translation and mRNA decay. Nat Rev Mol cell Biol 19:20–30
78. Caldararu O, Blundell TL, Kepp KP (2021) Three simple properties explain protein stability change upon mutation. J Chem Inf Model 61:1981–1988
79. Barrett CT, Neal HE, Edmonds K et al (2021) Effect of clinical isolate or cleavage site mutations in the SARS-CoV-2 spike protein on protein stability, cleavage, and cell-cell fusion. J Biol Chem. https://doi.org/10.1016/j.jbc.2021.100902
80. Teng S, Sobitan A, Rhoades R et al (2021) Systemic effects of missense mutations on SARS-CoV-2 spike glycoprotein stability and receptor-binding affinity. Brief Bioinform 22:1239–1253. https://doi.org/10.1093/bib/bbaa233
81. Mohammad T, Choudhury A, Habib I et al (2021) Genomic variations in the structural proteins of SARS-CoV-2 and their deleterious impact on pathogenesis: a comparative genomics approach. Front Cell Infect Microbiol. https://doi.org/10.3389/fcimb.2021.765039
82. Casalino L, Gaieb Z, Goldsmith JA et al (2020) Beyond shielding: the roles of Glycans in the SARS-CoV-2 spike protein. ACS Cent Sci 6:1722–1734. https://doi.org/10.1021/acscentsci.0c01056
83. Phillips PC (2008) Epistasis—the essential role of gene interactions in the structure and evolution of genetic systems. Nat Rev Genet 9:855–867
84. Ramanathan M, Ferguson ID, Miao W, Khavari PA (2021) SARS-CoV-2 B.1.1.7 and B.1.351 spike variants bind human ACE2 with increased affinity. Lancet Infect Dis. https://doi.org/10.1016/S1473-3099(21)00262-0
85. Mannar D, Saville JW, Zhu X et al (2022) SARS-CoV-2 Omicron variant: antibody evasion and cryo-EM structure of spike protein ACE2 complex. Science 375:760–764. https://doi.org/10.1126/science.abn7760
86. Zeldovich KB, Chen P, Shakhnovich EI (2007) Protein stability imposes limits on organism complexity and speed of molecular evolution. Proc Natl Acad Sci U S A 104:16152–16157. https://doi.org/10.1073/pnas.0705366104
87. Dasmeh P, Serohijos AWR, Kepp KP, Shakhnovich EI (2014) The influence of selection for protein stability on dN/dS estimations. Genome Biol Evol 6:2956–2967. https://doi.org/10.1093/gbe/evu223
88. Greaney AJ, Starr TN, Gilchuk P et al (2021) Complete mapping of mutations to the SARS-CoV-2 spike receptor-binding domain that escape antibody recognition. Cell Host Microbe 29:44–57
89. Starr TN, Greaney AJ, Dingens AS, Bloom JD (2021) Complete map of SARS-CoV-2 RBD mutations that escape the monoclonal antibody LY-CoV555 and its cocktail with LY-CoV016. Cell Reports Med 2:100255
90. Reetz MT (2013) The importance of additive and non-additive mutational effects in protein engineering. Angew Chemie Int Ed 52:2658–2666
91. Breen MS, Kemena C, Vlasov PK et al (2012) Epistasis as the primary factor in molecular evolution. Nature 490:535–538
92. Hopf TA, Ingraham JB, Poelwijk FJ et al (2017) Mutation effects predicted from sequence co-variation. Nat Biotechnol 35:128–135. https://doi.org/10.1038/nbt.3769
93. Rochman ND, Faure G, Wolf YI et al (2022) Epistasis at the SARS-CoV-2 receptor-binding domain interface and the propitiously boring implications for vaccine escape. MBio. https://doi.org/10.1128/mbio.00135-22

Publisher's Note Springer Nature remains neutral with regard to jurisdictional claims in published maps and institutional affiliations.